# INTRODUCTION TO RESIDUAL STRESS

**Eckard Macherauch**

*Institut für Werkstoffkunde I, Universität Karlsruhe (TH), FRG*

## INTRODUCTORY REMARKS

Residual stresses are self-equilibrating stresses existing in materials or components under uniform temperature conditions. It is well established that principally no materials and no components or structures of technical importance exist free of residual stresses. Such stresses always are produced if regions of a material are elastically or plastically inhomogeneously deformed in such a permanent manner that incompatibilities of the state of deformation occur. In materials, components and structures a great variety of residual stress states may exist due to various technological treatments and manufacturing processes.

If parts bearing residual stresses are externally loaded the total stress state is always composed of the loading stresses and the residual stresses. Consequently, residual stresses are of considerable interest and importance for both engineers and scientists. However, since the first quantitative reference to residual stresses [1] in 1841 up to now such a large number of contributions to this important field has been published [see e.g. 2-10], that assumedly nobody is really able to overview all details and facets of it. Therefore a handbook of this kind seems to be useful to present material scientists and engineers the actual state of knowledge about residual stresses, to give an advanced understanding of their origins, measurements, effects and evaluations and to make familiar with certain recent developments.

Residual stresses can have both detrimental or favourable consequences for the materials behaviour under certain conditions. The experiences reach from the explosion of heat-treated steel shafts lying unloaded on stock up to the increase of fatigue strength of parts due to mechanical or thermochemical surface treatments. Now as before, however, the actual knowledge about residual stresses is mostly scarce. In general, relatively expensive measurements or calculations are necessary to establish quantitative data of residual stress states. As a consequence in most cases in materials science and engineering residual stresses have not or have only qualitatively been taken into account in assessing physical and/or mechanical properties and service behaviour of materials, components and structures. Now as before, designers, engineers and material scientists very often use the term residual stresses as a mostly uncontrollable argument in the case of unexpected failure of technical parts. However, for the time being the situation is changing dramatically. Worldwide particular efforts are initiated in order to solve the various problems related to residual stresses

[see e.g. 5-10]. In recent years important improvements of the experimental methods as well as of the theoretical background have been achieved. Actually, designers are more than ever using the benefits of residual stresses. In order to maintain high qualifications in engineering education particular postgradiate and other special courses summarize important fundamental aspects of residual stresses and their application in a systematic manner.

The specific purpose of the introduction to this handbook is to comment on the nature, the generation, the measurement, the calculation, the effects and the assessment of residual stresses in a stimulating rather than in an overviewing way. It is intended to present some basic informations and to illustrate exemplarily the complex situation in the field of residual stresses.

## DEFINITIONS OF RESIDUAL STRESSES

Since residual stresses are self-equilibrating stresses, the resultant force and the resultant moment produced by them must be zero. An appropriate and standardized system of designations classifies three different kinds of residual stresses, called residual stresses of the 1st, 2nd and 3rd kind. Using the term "homogeneous" for "constant in magnitude and direction" the following definitions hold [11]:

- Residual stresses of the 1st kind are nearly homogeneous across large areas, say several grains, of a material and are in equilibrium over the bulk of the material. Every interference in the equilibrium of forces and moments of a volume containing 1st kind residual stresses will change its dimensions.

- Residual stresses of the 2nd kind are nearly homogeneous across microscopic areas, say one grain or parts of a grain, of a material and are equilibrated across a sufficient number of grains. Macroscopic changes of the dimensions of a volume comprising 2nd kind residual stresses may only be observed if distinct disturbances of this equilibrium will happen.

- Residual stresses of the 3rd kind are inhomogeneous across submicroscopic areas of a material, say some atomic distances within a grain and are equilibrated across small parts of a grain. No macroscopic changes of the dimensions of the stressed material will happen if this equilibrium is disturbed.

It can be shown that these definitions are sufficient to describe all residual stress states occurring in technical parts if mechanical effects of non-mechanical influences are absent. Usually, a superposition of residual stresses of the 1st, 2nd and 3rd kind determines the total residual stress acting at a particular point of a material, a component or a structural part. Figure 1 illustrates schematically a possible local superposition of the three different kinds of residual stresses. The y-component of the total residual stress is drawn as a function of x for y = constant and is locally given by

$$\sigma^{RS} = \sigma^{RS,I} + \sigma^{RS,II} + \sigma^{RS,III} \tag{1}$$

The different kinds of residual stresses are

$$\sigma^{RS,I} = \left| \frac{\int \sigma^{RS} dA}{\int dA} \right| \quad \text{at many grains } nA_K = A \tag{2}$$

$$\sigma^{RS,II} = \left| \frac{\int \sigma^{RS} dA_K}{\int dA_K} \right| - \sigma^{RS,I} \quad \text{at one grain } A_K \tag{3}$$

$$\sigma^{RS,III} = [\sigma^{RS} - (\sigma^{RS,I} + \sigma^{RS,II})]\Big|_{\text{at a point x of a grain}} \tag{4}$$

The macroscopic equilibrium of the forces with respect to 1st kind residual stresses for any plane section area A of the whole body requires

$$\int_A \sigma^{RS,I}\, dA = 0 \tag{5}$$

and the equilibrium of the moments with respect to an arbitrary reference line in the section area A demands

$$\int_A \sigma^{RS,I}\, r\, dA = 0 \tag{6}$$

r is the reference line distance of an element dA of the area A. Analogically, for the equilibrium of 2nd kind residual stresses the last two equations are valid with $A = nA_K$, where $A_K$ is the mean grain area and n an arbitrary large number. In the case of 3rd kind residual stresses A is $A_K$.

The classification of residual stresses discussed corresponds with the commonly used subdivision of residual stresses into macro residual stresses and micro residual stresses. Macro residual stresses are 1st kind residual stresses. Mostly, only this type of residual stresses is considered if engineers discuss problems and effects related to residual stresses. Micro residual stresses on the other hand are very often regarded as a combination of residual stresses of the 2nd and 3rd kind.

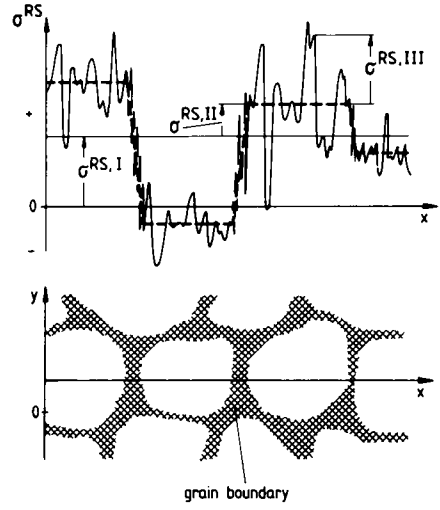


Fig. 1 Total residual stress distribution along several grains of a polycrystal (schematically) and their separation in 1st, 2nd and 3rd kind residual stresses.

## CHARACTERISTIC EXAMPLES OF RESIDUAL STRESS STATES

### 1st Kind Residual Stresses

Many processes exist generating residual stresses of the 1st kind with different magnitudes and distributions in materials, components and structures, e.g. machining, forming, joining, heat-treating etc. Characteristic examples are collected in Table 1. Any treatment causing inhomogeneously distributed elastic or plastic deformations and thus creating strain incompatibilities in between adjacent parts of a body produces 1st kind residual stresses. In all cases the resulting residual stress states strongly depend on the existing geometrical conditions and on the parameters of the applied treatments respectively processes. Also as a consequence of simple elastic-plastic loadings macro residual stresses occur, e.g. in the case of elastic-plastic bending and elastic-plastic torsion of smooth or notched bars. Some typical examples of 1st kind residual stress states will shortly be reviewed.

TABLE 1

| main groups | sub groups |
|---|---|
| machining residual stresses | grinding, turning, milling, planing, drilling } residual stresses |
| joining residual stresses | welding, soldering, brazing, adhering } residual stresses |
| founding residual stresses | |
| forming residual stresses | rolling, drawing, forging, pressing, spinning, shot peening } residual stresses |
| heat-treating residual stresses | quenching, transformation hardening, case hardening, nitriding } residual stresses |
| coating residual stresses | cladding, spraying, electroplating, plating, galvanizing } residual stresses |

In the case of elastic-plastic torsion of a cylindrical shaft the resulting residual shear stresses after unloading can be approximately estimated by the assumption that unloading is accompanied by elastic deformations only. Due to the elastic-plastic deformation state of the outer parts of the shaft, as Fig. 2 illustrates, the actual loading stresses $\tau^{LS}(r)$ are not linearly distributed along the radius. On the other hand a fictitious linear shear stress distribution $\tau^{*}(r)$, which would occur if the torsion moment would lead to elastic deformations only, can be calculated. The difference

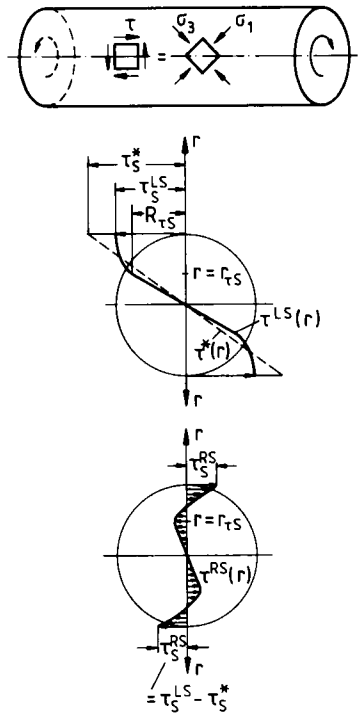


Fig. 2 Generation of shearing residual stresses due to elastic-plastic torsion of a cylindrical bar.

$$\tau^{LS}(r) - \tau^{*}(r) = \tau^{RS}(r) \tag{7}$$

yields the residual shear stress distribution after unloading. As can be seen from the graph in the lower part in Fig. 2 residual shear stresses of opposite signs occur in the outer and in the inner part of the shaft. The surface residual shear stress is opposite in sign to the loading shear stress.

Quenching in course of a heating-treating process may result in the generation of residual stresses of the 1st kind, if the quenching temperature is sufficiently high and the quenching process sufficiently rapid. During quenching of a metallic cylinder the outer parts cool down much faster than the interior. In the first stage of cooling this results in thermal stresses, being tensile near the surface and compressive near the centre of the cylinder both in axial and tangential directions and compressive in radial direction over the whole cross-section with exception of the very surface. If the equivalent stresses of the local thermal stress states reach the local yield strengths of the quenched material plastic deformations occur, which are inhomogeneously distributed. Due to these deformations, residual stresses remain after the thermal equilibrium has been reached.

Figure 3 shows the distributions of the time dependent longitudinal, tangential and radial thermal resp. residual stress components versus the radius of a plain carbon steel cylinder with a diameter of 50 mm and a length of 150 mm quenched from 600°C in ice water of 0°C [12]. The values hold for the middle part of the cylinder. The final residual stress distributions 60 s after

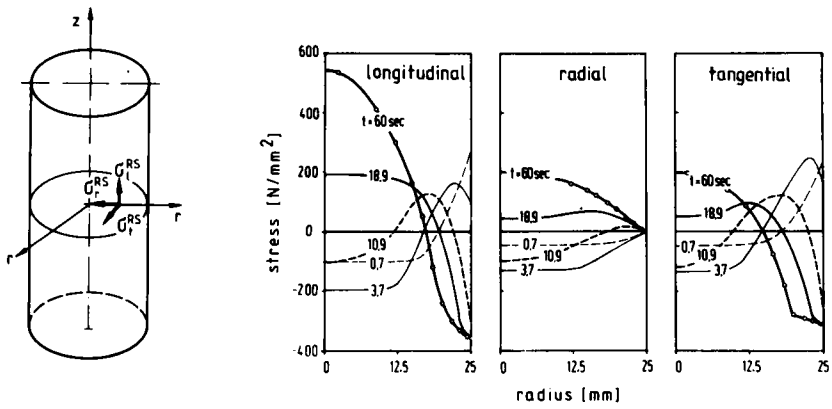


Fig. 3 Distribution of longitudinal, tangential and radial thermal resp. residual stresses in the cross section of a steel cylinder, waterquenched from 600°C to 0°C.

quenching are given by the thick solid lines. The very surface in the middle part of the cylinder contains compressive residual stresses in the longitudinal and tangential direction of about equal magnitude. In the core region of the cylinder a triaxial tensile residual stress state exists.

Other important sources of residual stresses are machining processes like turning, milling, grinding, planing etc.. In the surface layers of parts or components machined by these methods always combinations of cutting processes and inhomogeneous plastic deformation processes occur. Simultaneously friction processes create heat. The removal of material is in any case noticeably influenced by its mechanical and thermal properties, the kind and geometry of the cutting tool used and the cooling conditions. In total, machining is a multiparametric mechanical treatment which besides a distinct surface topography, always produces a characteristic workhardened surface state and a specific residual stress pattern in and beneath the machined surface. As an example, some characteristic results concerning the influence of different milling procedures on magnitude and sign of surface residual stresses of a plain carbon steel are grouped in Fig. 4. The stress components parallel ($\sigma_l$) and transverse ($\sigma_t$) to the milling direction are shown. As can be seen, up-cut and down-cut milling produce nearly the same magnitudes of residual stresses but opposite signs in the very surface of the machined samples. Also face-milling with the axis of the tool inclined resp. perpendicular to the surface of the machined parts creates opposite signs of surface residual stresses.

One of the most important technological methods of producing compressive residual stresses in and beneath the surface of structural parts is shot peening. It is a high velocity bombarding of the surface of a material with shots of steels, glass or ceramics. Shot peening produces in most cases residual stress distributions as illustrated in Fig. 5 for steel parts peened with two different coverages, shot velocities and mean shot diameters. Maximum compressive residual stresses develop in certain distances from the surface. The thickness of the surface layer with compressive residual stresses depends on the hardness and the grain size of the shots, the kinetic energy transferred by the shots to the surface of the material, the coverage and the tensile strength of the peened part.

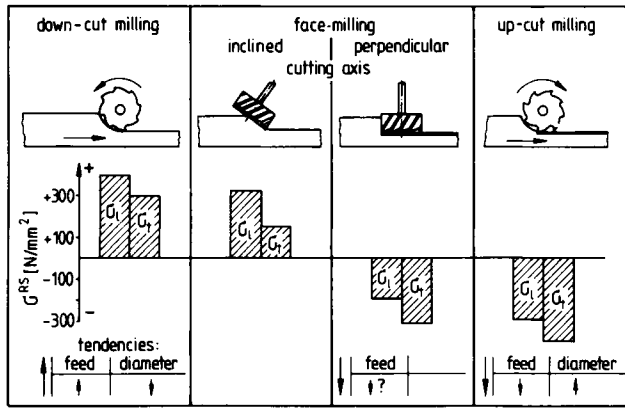


Fig. 4 Signs and magnitudes of surface residual stresses of differently milled plain carbon steel specimens due to variation of the machining parameters.

2nd Kind Residual Stresses

Residual stress states which can entirely be attributed to 2nd kind residual stresses are very rare. However, examples can be given for homogeneous as well as for heterogeneous materials which describe such states at least approximately. Homogeneous materials with a pronounced anisotropy of the yield strength and work hardening of their grains, show residual grain stresses of different magnitudes after uniaxial elastic-plastic tensile deformation. The sign of the grain stresses depends on the orientation of the grains with respect to the deformation direction. All grains with a larger (smaller) yield strength $R_{eS}$ than the average yield strength $\bar{R}_{eS}$ of the material are sources of tensile (compressive) residual stresses. The residual stresses are in equilibrium over a sufficiently large number of grains. Such conclusions can be derived from the simple model illustrated in Fig. 6, which assumes that all grains behave like equally strained parts with the same elastic response but orientation dependent yield strengths and workhardening abilities. Apart from the workhardening curve of a grain, which behaves like the bulk material, also the workhardening curves of the grains with the largest and the smallest yield strength (and workhardening) are drawn schematically. The workhardening curves of all other grains are considered lying between these boundary curves. Unloading after a certain extent of total deformation develops residual stresses, whereby the grains with the largest resp. the smallest yield stresses receive the largest 2nd kind tensile residual stresses $\sigma^{RS}$ resp. the largest 2nd kind compressive residual stresses $\sigma^{RS}_{min}$.

Other characteristic examples for 2nd kind residual stress states are documented by the data shown in Fig. 7. The stresses in the grains of several well-annealed heterogeneous tungsten carbide-cobalt-alloys are plotted as a function of the volume content of cobalt. Due to the differences in the thermal expansion coefficients of both phases, the cobalt grains are subjected to tensile residual stresses (indicated by dots) which are equilibrated by compressive residual stresses in the tungsten carbide grains (indicated by circles). The necessary equilibrium of the residual grain stresses can be shown approximately (indicated by crosses) using the volume contents of both phases and applying a simple mixture rule [13].

In particular cases during heat-treatment of materials incomplete transformations may occur. Consequently, besides grains of the newly developed phase the

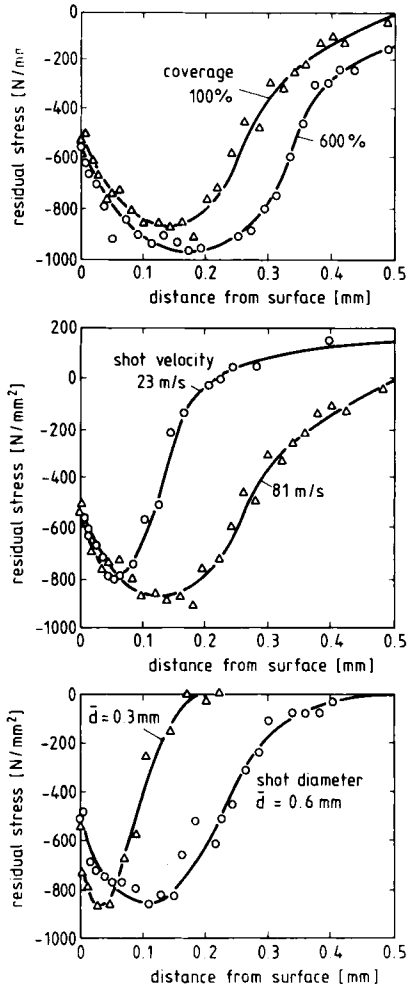


Fig. 5 Residual stresses versus distance from the surface of quenched and tempered steel specimens, shot peened with different velocities (top), coverages (middle) and shot sizes (bottom).

material also contains grains of the initial phase. If the specific volumes of both phases differ, residual grain stresses develop. The most important examples in this respect are martensitically transformed steel specimens (with a relatively high content of carbon or distinct alloying elements), which are composed of grains of martensite and retained austenite. Since the specific volume of martensite is always larger than that of retained austenite residual stresses of the 2nd kind occur.

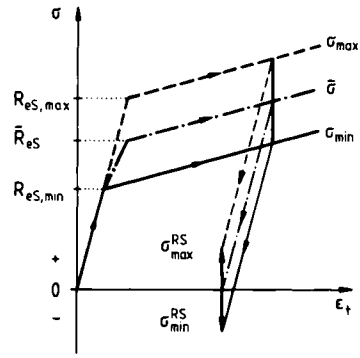


Fig. 6 Development of 2nd kind residual stresses during elastic-plastic tensile deformation of a polycrystal as a consequence of the anisotropy of yield strength and work hardening of the grains (schematically).

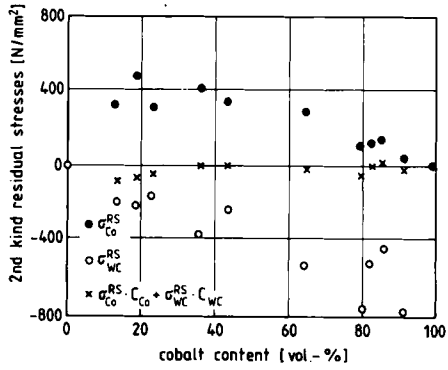


Fig. 7 2nd kind residual stresses in the WC- and Co-grains of a heterogeneous WC-Co-alloy cooled to room temperature.

## 3rd Kind Residual Stresses

Residual stress states of the 3rd kind are connected with all types of lattice imperfections, occurring in the interior of the grains of homogeneous or heterogeneous polycrystals as well as at the grain boundaries. Important examples are the residual stress fields accompanying dislocations [see e.g. 14]. In Fig. 8 the residual stress field of an edge dislocation is illustrated schematically. The residual shear stresses $\tau^{RS}_{xy} = \tau^{RS}_{yx}$ and the residual normal stresses $\sigma^{RS}_{yy}$ change their signs if the lines $y = \pm x$ are passed. Above resp. beneath the slip plane compressive resp. tensile residual normal stresses $\sigma^{RS}_{xx}$ occur. All stress components decrease inversely with the distance to the centre of the dislocation. Figure 9 shows quantitatively the distributions of the components $\sigma^{RS}_{xx}$ and $\tau^{RS}_{xy}$ around the centre of an edge dislocation. Since in most materials of technical importance relatively large dislocation densities occur, the stress fields of the single dislocations superimpose within the grains and complex residual stress states occur. Any changes in the density of dislocations, e.g. due to plastic deformation, are connected with changes

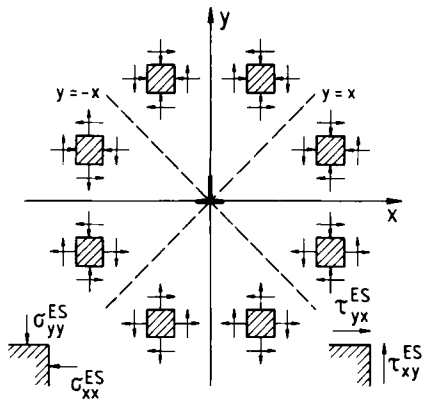


Fig. 8 3rd kind residual stress field around an edge dislocation, schematically.

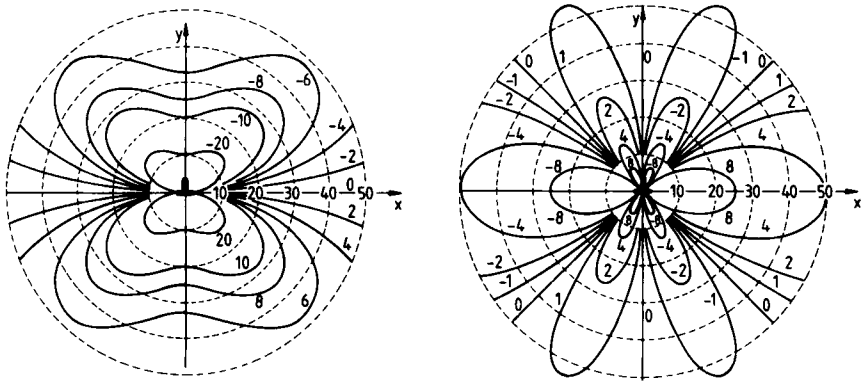


Fig. 9 Distribution of 3rd kind residual stress components $\sigma^{RS}_{xx}$ and $\tau^{RS}_{xy}$ around an edge dislocation. Unit of distance: Burgers vector, unit of stresses: $G/400\pi\ (1-\nu)$ with G shear modulus and $\nu$ Poisson's ratio.

in the residual stress state. Also changes in the arrangement of the dislocations will lead to changes in the resulting 3rd kind residual stresses.

## Superposition of Different Kinds of Residual Stresses

The 1st, 2nd and 3rd kind residual stress states described in the preceding chapters display abstractions, since in any individual case only distinct kinds of stresses are considered. In reality all technical parts or components holding 1st kind residual stresses due to previous technological treatments also bear 2nd and 3rd kind residual stresses. Typical examples are hardened steel axles and milled metal sheets. Hardened axles manufactured from a low-alloy steel show a superposition of quenching and transformation residual stresses of the 1st kind and, if macroscopic distortions were cancelled by straightening, also 1st kind deformation residual stresses. The different specific volumes of austenite and martensite and the different coefficients of thermal expansion of martensite, retained austenite and carbides lead to residual stresses of the 2nd kind. As a consequence of elastic anisotropy as well as of yield strength anisotropy also 2nd kind residual stresses may occur. Furthermore

the high dislocation density and the interstitially dissolved carbon atoms in the martensite cause strong 3rd kind residual stresses. In a similar way the mental separation of the different kinds of residual stresses in the above-mentioned milled metal sheets can be carried out.

If material states free of 1st kind residual stresses should be produced by annealing at sufficient high temperatures also 2nd and 3rd kind residual stresses are reduced. However, all material states free of 1st kind residual stresses are always influenced by 3rd kind residual stresses, often also by 2nd kind residual stresses. As already stated, constructional parts, which are residual stress free in the true sense of the word, can consequently never be achieved.

## MEASUREMENT OF RESIDUAL STRESSES

As already mentioned, the actual stress state of any material, component or structure is determined by the superposition of loading stresses and residual stresses. Nowadays, sophisticated methods available in the field of experimental and theoretical stress analysis allow in almost all cases the appropriate determination of permissible loading stresses. On the other hand, however, the accurate evaluation of acting residual stresses includes various problems. Cheap, simple and reliable methods for the determination of residual stress distributions do not exist, although various methods of measuring residual stresses have been developed in course of time [see e.g. 5-10, 15-19]. Table 2 gives a rough survey about the most important methods, the measured quantities, from which distinct kinds of residual streses can be determined and the destructive resp. non-destructive character of the single measuring procedures. According to their nature residual stresses can be determined

- from macroscopic strains released while material is removed from parts loaded by residual stresses. This is the base of all mechanical methods;
- from residual lattice strain distributions. This is the base of X-ray and neutron diffraction methods;
- from their effects on distinct physical properties. This is the base of ultrasonic and magnetic methods.

At the present time the most widely applied methods are X-ray diffraction and mechanical strain gauge procedures. The X-ray method is the only non-destructive method existing for the measurement of surface residual stresses. Since homogeneous lattice strains of distinct oriented sets of grains are measured,

TABLE 2

| Method | Measured quantities | Residual stresses determined | Character |
|---|---|---|---|
| mechanical | macroscopic surface strains | 1st kind | destructive |
| X-ray diffraction | homogeneous lattice strains | 1st+2nd kind | non-destructive (surface) |
| neutron diffraction | homogeneous lattice strains | 1st+2nd kind | non-destructive |
| ultrasonics | e.g. t! of flight differences of shear waves | 1st+2nd+3rd kind | non-destructive |
| magnetic | e.g. Barkhausen-noiseamplitudes | 1st+2nd+3rd kind | non-destructive |

always residual stresses of the 1st and 2nd kind are determined. All mechanical methods are destructive. The disadvantage of these methods destroying the parts, which have to be analysed, frequently seems to be compensated by the fact that only macro residual stresses are registrated and that the application in some cases is very simple. The neutron-diffraction method allows the non-destructive analysis of residual stress states in the interior of parts. Residual stresses of the 1st and 2nd kind are measured. Since the measured volumes are relatively large, existing 2nd kind residual stresses mostly are equilibrated and pure 1st kind residual stresses are determined. Finally, it should be noted that promising progresses were achieved in recent years with ultrasonic and magnetic residual stress measuring techniques. Significant research activities are well on their way to improve the practical applicabilities of these procedures.

In the following, only a few comments will be given on the above-mentioned procedures for the determination of residual stresses concerning their principles, advantages and limitations. All mechanical techniques to determine residual stresses are based either on the measurement of macroscopic strains released due to removing stressed materials by mechanical or etching treatments or on the measurement of shape changes due to cutting stressed material. As an example of a modern measuring technique the upper part of Fig. 10 shows the requirements for the ring coring method [20], which measures changes of surface strains with rosettes of strain gauges (indicated as RSG) during milling a ring shaped slot of distinct dimensions in the part of interest. From the strains measured, surface residual stresses as well as residual stress distributions beneath the surface can be calculated. As a characteristic result the lower part of Fig. 10 shows the distributions of axial and tangential surface residual stresses for a generator shaft with a diameter of 1.80 m and a length of 6.4 m [21]. As can be seen, only small quantities of surface residual stresses occur.

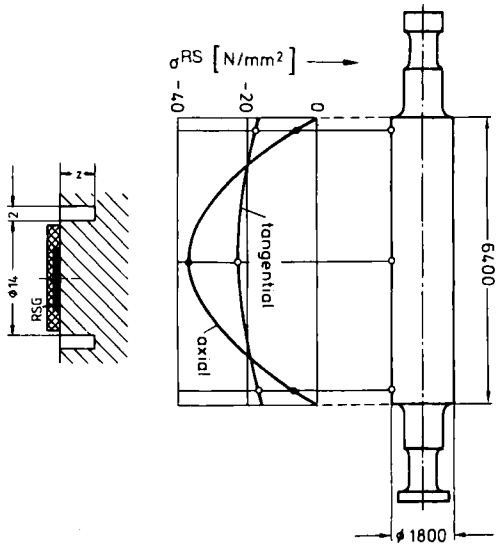


Fig. 10 Distribution of axial and tangential residual stresses of a generator axle determined with the ring coring method.

Besides the described technique also other mechanical procedures like e.g. the classical boring-out or cutting-off methods, the hole drilling method and the

beam deflection method frequently are used [15,16]. In all these cases portions of the residually stressed components are cut away and the strains appertaining to the disturbance of the original equilibrium of the residual stress state are measured. From the measured strains conclusions are drawn about sign, magnitude and distribution of the residual stresses. All destructive techniques are time consuming and show deficiencies with respect to the resolving power, if steep gradients of residual stresses occur. Furthermore, some of the developed methods can only be applied without analytical difficulties, as long as the shape of a component to be analysed agrees with that quantitative procedures for calculating the residual stresses from the theory of elasticity have been derived for. Generally, residual stresses in components being actually in service cannot be analysed with mechanical methods. This imposes a further limitation for their practical use. Exceptions in this respect are the hole drilling and the ring coring method in such cases, where the holes and the ring slots necessary for the measurements are very small and consequently they may be considered as non-destructive.

The X-ray diffraction method of residual stress analysis is basically restricted to surface stress determinations, since the applicable X-ray wave lengths have only very small penetration depths in most anorganic materials. Always the shifts of interference lines are measured which are proportional to homogeneous lattice strains determined in equal crystallographic directions of many grains in and near the surface of the investigated materials. According to the theory of elasticity any biaxial 1st kind surface residual stress state reveals strains, which are linearly dependent on $\sin^2\psi$ in all azimuths of the appertaining deformation ellipsoid. Consequently in such cases the so-called $\sin^2\psi$-method [22] can be applied for residual stress determinations by X-ray diffraction, measuring homogeneous lattice strains in various oblique angles $\psi$ against the surface normal in appropriate azimuth planes of the surface area of interest. Nowadays such measurements are perforemd in special computer-controlled X-ray diffractometers, which perform data processing, plot graphs of the existing residual lattice strain distributions and calculate signs and magnitudes of the residual stresses causing these distributions automatically. Stationary as well as mobile diffractometers are available. The choice of $\psi$-diffractometers [23] yields special advantages. The measuring time for single residual stress components depend on the material states to be analysed and may reach from a few minutes up to about hours. A typical result for a complete X-ray analysis of the surface residual stress state of a material is shown in Fig. 11. In 36 azimuths the surface residual stress components of a rolled armco-iron sheet were determined measuring in any azimuth in 8 $\psi$-directions the positions of {721}/{633}/{552}-interference lines with Mo-K$\alpha$-radiation. The total measurements for one component were carried out in about 2.5 hours. The principal residual stresses parallel and perpendicular to the rolling directions are $\sigma_1$ = -202 N/mm² and $\sigma_2$ = -173 N/mm², respectively [24].

An important feature of X-ray lattice strain measurements is the fact, that always the combined influence of 1st and 2nd kind residual stresses acting in the irradiated material volume is determined. Therefore sometimes problems of interpretation of the measured quantities occur. According to experience in special cases also 2nd kind residual stresses produce lattice strains linearly distributed versus $\sin^2\psi$, superposed on lattice strains due to 1st kind residual stresses. This is observed for example in uniaxially deformed plain carbon steel specimens. An example is shown in Fig. 12 [25]. In this particular case the separation of 1st and 2nd kind residual stresses was achieved by combining the $\sin^2\psi$-method with an electrolytic method of removal of parts of the object being examined. The experimentally determined residual stress distribution over the diameter of the cylindrical tensile specimen (left part of Fig. 12) results from the superposition of locally changing 1st kind residual stresses (middle part of Fig. 12) and of constant 2nd kind residual stresses (right part of Fig. 12). The values hold for a 6% plastically deformed tensile specimen. Obviously in all cases, where doubts occur about the meaning of measured lattice

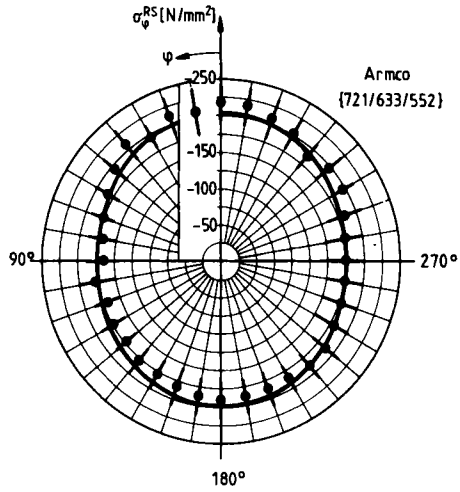


Fig. 11 Residual surface stress distribution of a 78% cold-rolled armco iron sheet determined by X-ray diffraction at {721}/{633}/{552}-lattice planes.

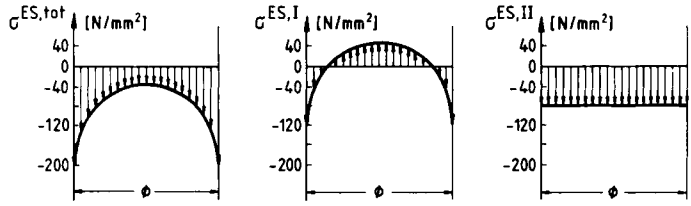


Fig. 12 Distribution of longitudinal residual stresses along the diameter of a 6% tensile deformed steel specimen determined by X-rays. Total residual stresses (left), 1st kind residual stresses (middle) and 2nd kind residual stresses (right).

strain distributions in terms of residual stresses, the simultaneous application of X-ray and mechanical methods for residual stress analysis seems to be useful.

Two examples, published recently, should be presented. Figure 13 shows the distribution of the longitudinal residual stresses versus the radius of an ice-water quenched nickel-steel cylinder determined by two mechanical methods and the X-ray method [26]. As can be seen, the comparative measurements agree excellently. Another example, which reveals marked differences between X-ray and mechanical residual stress measurements is illustrated in Fig. 14. The residual stress distributions beneath the surface of ground specimens of a ball bearing steel are considered. The surface and subsurface residual stresses parallel to the grinding direction determined by X-rays are considerably higher than the values derived from a mechanical deflection method. At least in a qualitative sense both methods deliver similar stress distribution. The authors [27] state, that the observed differences "may have their source in the completely different measurement techniques or in the machining process, or in both of these". Obviously further investigations are needed to outline the roots of such differences.

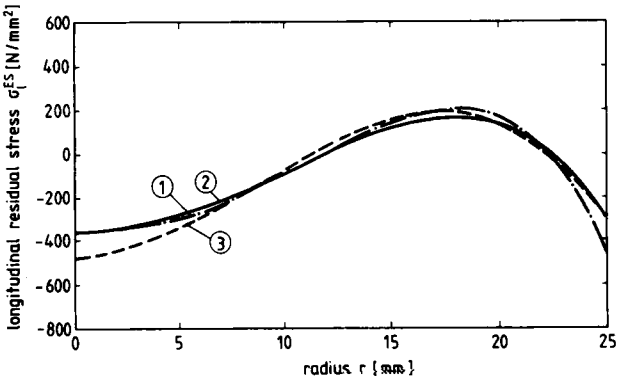


Fig. 13 Longitudinal residual stresses versus radius of a quenched nickel-steel cylinder (600°C → 0°C, diameter 50 mm, length 200 mm) measured by (1) boring-out method, (2) combined boring-out and cutting-off method, (3) X-ray method.

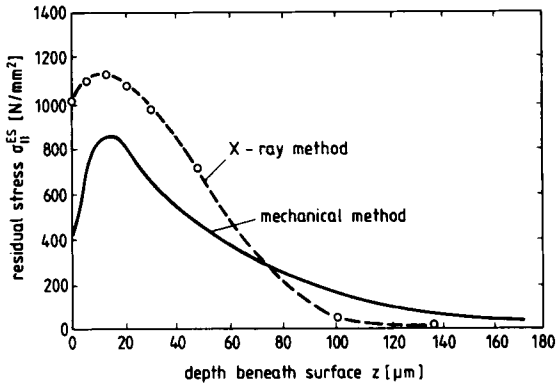


Fig. 14 Residual stress distributions of a ground ball-bearing steel determined mechanically and by X-rays.

Very recently, also in the case of heavily texturized steel sheets the effects of 1st and 2nd kind residual stresses on the lattice strain distributions determined from the shifts of interference lines with low {hkl}-indices were separated [24]. In such cases non-linearly distributed lattice strains versus $\sin^2\psi$ are observed. However, by measuring multiple interference lines with large {hkl}-indices strains of a much higher number of grains or parts of grains are obtained. By such measurements the 2nd kind residual stress effects due to the influence of elastic anisotropy are to a certain extent averaged out and quasi-linear distributions of the lattice strains versus $\sin^2\psi$ are found. Thus, by the aid of high indexed multiple interference lines surface residual stress states of the 1st kind can be determined at least approximately. Combining these results with those, gained from interference lines with low indices, information about deformation-induced 2nd kind residual stresses can be derived. A useful tool in this respect are lattice deformation pole-figures, introduced recently [28]. As an example, Fig. 15 shows the 2nd kind lattice deformation

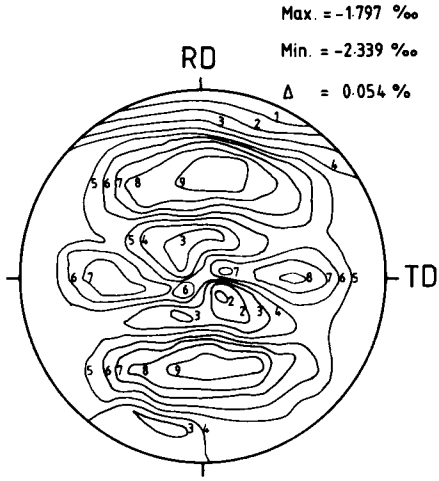


Fig. 15 2nd kind deformation pole figure of a 78% cold-rolled armco iron sheet determined by X-ray diffraction at {211}-lattice planes. RD rolling direction, TD transverse direction.

pole-figure of a 78% cold rolled armco-iron sheet (carbon content 0.03 wt.-%) measured with Cr-Kα-radiation on {211}-planes of ferrite.

Meanwhile the difficult interpretation of the residual lattice strain states of highly texturized materials, characterized by non-linearities of the homogeneous lattice strains versus $\sin^2\psi$ determined by low indices interference lines, has led to the proposal of several methods how to evaluate residual stresses from the measured data [7,29-32]. All these methods start with certain assumptions about the existing texture states and the effective elastic constants and result in complicated evaluation procedures that are less applicable for practical purposes. However, also in materials free of texture effects non-linear distributions of residual lattice strains can be observed, if measurements by X-ray diffraction are performed. Typical examples are depicted schematically in Fig. 16. Curved residual lattice strain distributions may occur, if strong gradients of residual stresses exist near the very surface of the materials being examined (middle part of Fig. 16). If the principal axes of the stress system are inclined to the axes of the sample co-ordinate system, shear stresses appear in the specimen surface, causing different interference line positions at $\psi$-angles of equal magnitude but opposite sign ($\psi$-splitting). Then, the strain distributions versus $\sin^2\psi$ are no longer linear but elliptical (right part of Fig. 16). In the examples mentioned more time and cost are needed for the evaluation of the residual stress states than in such cases, where the premises of the classical $\sin^2\psi$-method are fulfilled.

A very important feature of X-ray stress analysis is the possibility to determine residual stress states in very small volumes of surface material. Consequently residual stress determinations in the root of notches as well as near crack tips or generally spoken in surface areas with pronounced local changes in the residual stress state can be performed. As an example Fig. 17 shows the distribution of the surface residual stresses acting parallel and perpendicular to the bead in the middle part of electron-beam welded plates of a plain carbon steel with 0.32 wt.-% carbon [33]. High compressive residual stresses occur in the centre of the bead. Maximum tensile residual stresses develop in a certain distance to the bead at both sides of the weld.

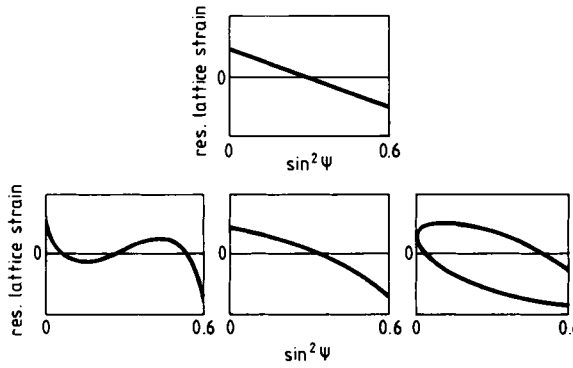


Fig. 16 Non-linear residual lattice strain distributions versus $\sin^2\psi$ caused by texture effects (left), steep stress gradient (middle) (schematically) and multi-axiality of near-surface residual stress state (right).

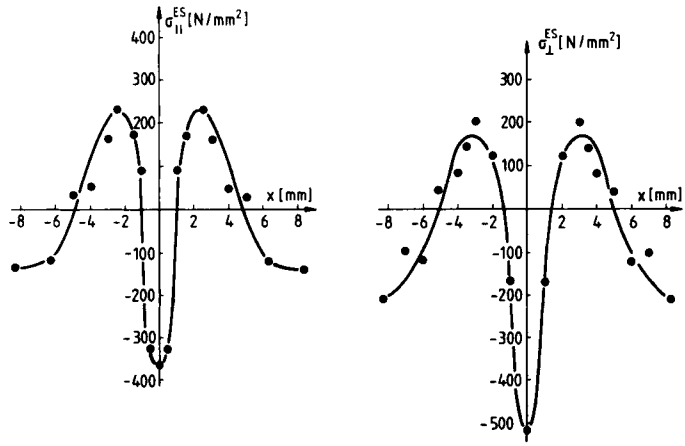


Fig. 17 Surface residual stresses parallel (left) and perpendicular (right) to the bead versus distance from the centre of the bead in the middle of electron-beam welded sheets.

Recent developments have shown that - if cases of too strong stress gradients are omitted - neutron diffraction offers excellent possibilities to determine non-destructively residual stress components in the interior of components [34-36]. In special cases three-dimensional stress profiles have accurately been measured. However the experimental expenditure is very large. A source of thermal neutrons must be provided, so that appropriate measurements only can be made, where e.g. nuclear reactors are available. In the meantime several successful residual stress evaluations by means of neutrons have been performed. Since neutron sources are relatively weak in comparison to X-ray sources,

relatively large volumes have to be measured. The smallest area for which accurate values have been published up to now, measures 1 x 1 x 10 mm. Thus, a great advantage of practically all neutron lattice strain measurements is the unlikeliness of measuring distinct effects of 2nd kind residual stresses. Mostly, mean values of the lattice strains due to residual stresses of the 1st kind are to be expected. In Fig. 18 the distribution of the tangential residual stresses of an autofrettaged thick-walled tube, determined by X-ray and neutron diffraction, are compared. As can be seen, good agreement exists although the neutron measurements were taken in the interior of the tube whereas the X-ray measurements were performed on a carefully prepared cross-section area of the tube.

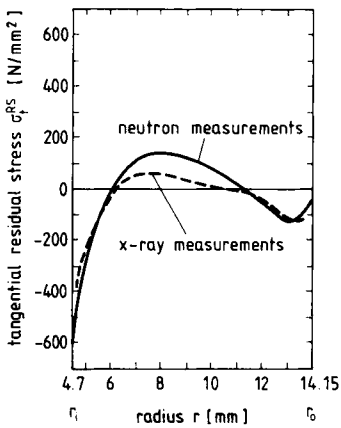


Fig. 18 Tangential residual stresses of an autofrettaged thick-walled tube determined by neutron diffraction and by X-ray diffraction.

The most promising methods for future residual stress analyses are based on the stress dependence of the velocities of ultrasonic waves in solid materials [6,9,18,19,25]. The occurring differences in velocities of longitudinal waves, polarized shear waves and Rayleigh surface waves can be related to residual stresses acting in the path traversed by the ultrasonic beam, if the high-order elastic constants of the material being investigated are known. These constants, which strongly depend on the actual state of the material of interest, must be determined in calibrating experiments. For the time being objective assessments of the capabilities, the limitation and the future development of the various ultrasonic possibilities of residual stress measurements are scarce. In spite of this several successful applications of ultrasonic methods to analyse internally stressed structural parts have been published. A typical result [37] is illustrated in Fig. 19. The picture shows the difference of the tangential and radial residual stresses in a textured saw blade versus the radius of the blade. Although differences between both methods arise, a satisfying agreement exists altogether.

## COMPUTATIONAL RESIDUAL STRESS ANALYSES

Besides improved experimental investigations of residual stresses the demand for analytical residual stress determination methods has grown in almost all technical disciplines in course of time. Several analytical methods to predict the 1st kind residual stress response of technologically treated components

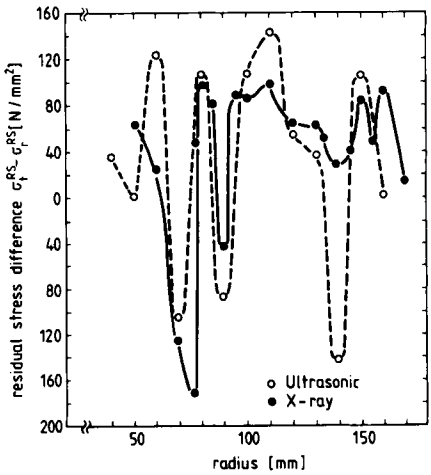


Fig. 19 Residual stresses of a saw blade determined by X-rays and ultrasonic waves.

were developed. Since the middle of the 1960s, when computers became widely available for computation purposes, modern numerical tools like the finite element method and the finite difference method were more and more applied in solving residual stress problems. Several specialized elastic-plastic finite element programs have been developed to analyse the generation of the residual stress states of various subjects. At present the main activities may be seen in the fields of welding, forming and heat-treating [see e.g. 38-47]. The formulation of mathematical models of such processes usually involves the consideration of various parameters. For example, the quantitative description of welding residual stresses demands the appropriate consideration of structural design parameters, welding procedures including kind of heat source, heat input, restraining conditions, etc., instationary temperature states, temperature dependence of thermal and mechanical properties including temperature-dependent stress- strain relationships and formulation of an arbitrary yield criterion. Considering residual stresses due to heat treating most of the factors mentioned have also to be taken into account as long as coolings occur without phase transformations. If transformation processes are involved as in rapid quenching of steel parts from high temperatures, all data about the formation and the properties of martensite have to be regarded, too.

Actually, the thermal and transformation processes during quenching as well as during welding are very fast. Therefore it is impossible to observe experimentally the development of stresses during such treatments. Modern computer simulations permit, however, to prolong the interesting time intervals of such processes in an arbitrary manner, allowing to investigate details which could not be studied up to now. Furthermore, the direct comparison of analytical predictions with experimentally determined residual stress data yields an objective control of the correctness of the applied computational procedures. In the past several analytical approaches have been developed to analyse, e.g.

- transient temperature and stress distributions as well as the final development of residual stresses and distortions due to different welding processes [48,49],

- the problem of crack growth in weld-induced residual stress fields [50],

- the residual stress pattern in autofrettaged cylindrical tubes and their redistribution due to notches or cracks [51],

- the generation of residual stress states in quenched parts with and without consideration of phase transformation processes [43-47],

- the development of residual stresses generated during the heat treatment of case carburized components [52],

- the quantitative evaluation of the residual stress states of induction hardened parts [53,54].

In the following three characteristic examples are presented which may illustrate recent activities in the field of computer-aided analytical predictions of 1st kind residual stresses. Figure 20 shows in the upper part the finite element mesh used for predicting the axial and hoop residual stresses in a two-pass girth-butt welded pipe (diameter approximately 315 mm, wall thickness approximately 4.6 mm). The middle and lower part of the figure depict for the inner surface of the pipe the calculated and the mechanically measured axial and hoop residual stresses in dependence on the distance from the centre of the weld. While a satisfying agreement between computed and measured axial residual stresses exist, marked discrepancies occur between calculated and experimental hoop residual stresses in larger distances from the edge of the weld. Also at the outer surface of the welded pipe the agreement between measurement and calculation is better for the axial than for the hoop residual stresses [48].

In the past decade several finite element programs have been developed [see e.g. 38, 40-47] for the calculation of residual stress states of quenched parts, including phase transformation processes and consequences of changes in the chemical composition due to thermochemical heat-treatments. Nowadays it is easily possible to describe quantitatively in dependence on time the local distortions and local thermal resp. transformation stresses during cooling as well as the final residual stress state after equalization of temperature of rapidly quenched components of not too complicated shape. Figure 21 shows a sequence of computer graphs, which visualize the development of the axial stresses of a steel cylinder water quenched from 600°C to 0°C [43]. Perpendicular to the z,r-plane (z is longitudinal, r radial axis at the middle of the cylinder) tensile stresses are plotted upwards and compressive stresses downwards. According to the boundary conditions, the axial stresses disappear at the free end of the cylinder. 0.7 s after starting quenching tensile stresses near the surface of the cylinder equilibrate compressive stresses in the interior. Later on (e.g. 10.9 s after quenching) as a consequence of inhomogeneous plastic deformations the sign of the thermal stresses in the outer part and afterwards also in the inner parts of the cylinder change and finally (18.9 s after quenching) tensile residual stresses in the core are equilibrated by compressive residual stresses near the cylinder surface. In Fig. 22 the calculated residual stress components of another steel cylinder of 100 mm length and 12 mm diameter, quenched from 680°C in water of 20°C are compared experimentally with surface stress values determined by X-ray diffraction. As can be seen, there is a very satisfying correspondence between calculated and measured stress values.

In the last years particular efforts were made to treat quantitatively the development of residual stresses as a consequence of the hardening of steels [40-47]. In the finite element computer programs used the thermoelastic-plastic behaviour of the parts during quenching was modelled with accurate consideration of the involved phase transformation processes. Important facts influencing the developing residual stress state of martensitically hardened parts are the interaction between actual stresses and transformation processes as well as the transformation plasticity, which accompanies the transition from austenite to martensite. Very recently the effects of transformation plasticity and stress-modified transformation kinetics have been taken into account by calculating

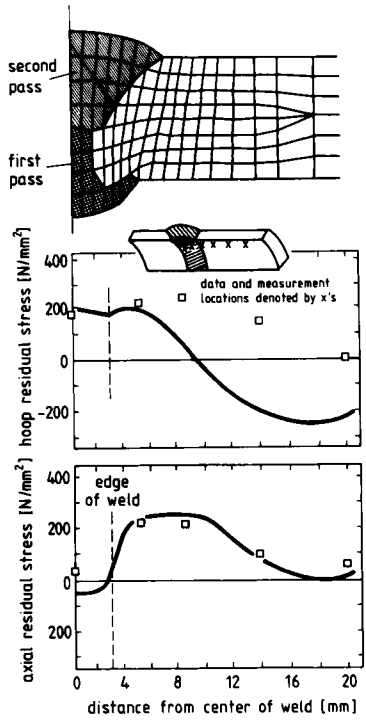


Fig. 20 Finite element mesh for computation of the residual stress state of a two-pass girth-butt welded pipe (upper part of the figure) and comparison of calculated and experimentally determined hoop (middle part of the figure) and axial residual stress distribution (lower part of the figure) at the inner surface of the welded pipe.

the residual stresses of a martensitically hardened cylinder of an alloyed steel [47]. Figure 23 allows the comparison of the calculated longitudinal residual stress distributions considering the mentioned effects with experimental results.

A further interesting field of computational residual stress determinations is induction hardening of steel specimens, which comprises electromagnetic heating and subsequent quenching. It is a frequently used heat-treatment method of great practical importance. Figure 24 shows calculated distributions of longitudinal (left) and tangential (right) residual stresses over the radius of cylinders of a plain carbon steel (German grade Ck 45) with diameters of 30, 60 and 120 mm [53]. In all cases the same conditions for induction heating and subsequent quenching were assumed. In the heating stage surface layers of 1 mm thickness were heated with a source power density of 2.4 $W/mm^3$. As a consequence of locally different amounts and distributions of plastic deformations residual stress states occur with pronounced differences in sign and magnitude of residual stresses in the surface and in the interior of the cylindrical specimens. Obviously, induction hardening with comparable heat input results in a distinct size-effect regarding the residual stress distributions of parts with different dimensions.

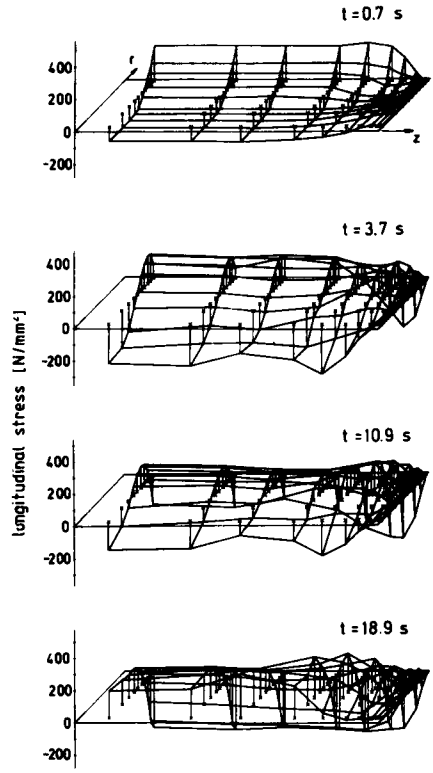


Fig. 21 Generation of longitudinal thermal stresses in a steel cylinder of 300 mm length and 15 mm diameter after quenching from 600°C to 0°C in dependence on time. The distribution at the bottom of the figure describes the quenching residual stress state.

## ASSESSING ASPECTS OF RESIDUAL STRESSES

The safety of statically and/or cyclically loaded components is of fundamental concern in technology. Consequently, technical components have to be designed and fabricated with sufficient reliability. In dimensioning constructional parts the relation between loading stresses and strength response of the material being used is almost entirely considered under complete ignoration of residual stresses. However, the local stresses in a material/component/structure are always the sum of residual stresses and stresses due to external forces and moments. Consequently, residual stresses have to be taken into account if reliable and safe constructions should be performed [see e.g. 5,9]. As all residual stresses influence the service behaviour of materials/components/structures, it is of particular interest for engineers and designers to know where benefits of residual stresses actually occur and can be utilized successfully. One large deficiency in respect to a systematic discussion of the consequences of residual stresses on service behaviour is the fact, that sufficient information about the real existing residual stress states is most unavailable. In actual cases, residual stresses severely depend on fabrication parameters as well as on process variables of the technological treatments being applied. Any manufacturing process produces individual residual stress

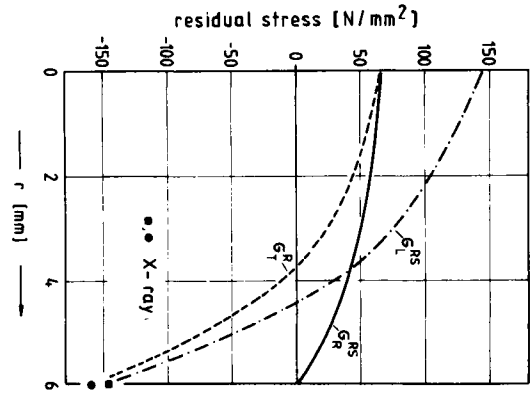


Fig. 22 Calculated distributions of longitudinal, tangential and radial residual stresses in a steel cylinder (100 mm length, 12 mm diameter) after quenching from 680°C to 20°C and experimentally determined longitudinal and tangential surface residual stresses.

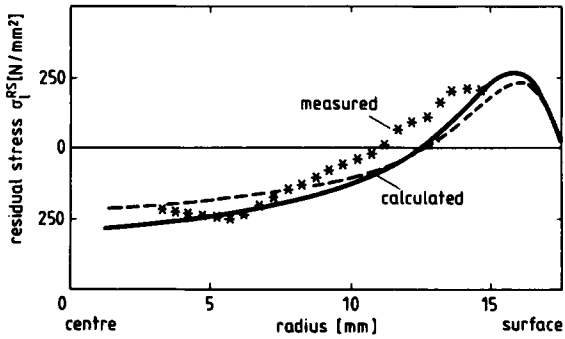


Fig. 23 Calculated distributions of longitudinal residual stresses in a cylinder of 60 NiCr 10 3 taking into consideration —— stress transformation interactions and transformation plasticity, --- transformation plasticity. The cylinder with a length of 105 mm and a diameter of 35 mm was water-quenched from 900°C to 20°C. The experimentally determined stress values are denoted by ****.

patterns in a given structural component. Consequently, the correct assessment and optimized use of residual stresses in engineering create a number of problems. For example in welding as a consequence of the large amount of heat necessarily complex thermal stress states develop, which produce inhomogeneous plastic deformations and often cause cracking. The most serious problems associated

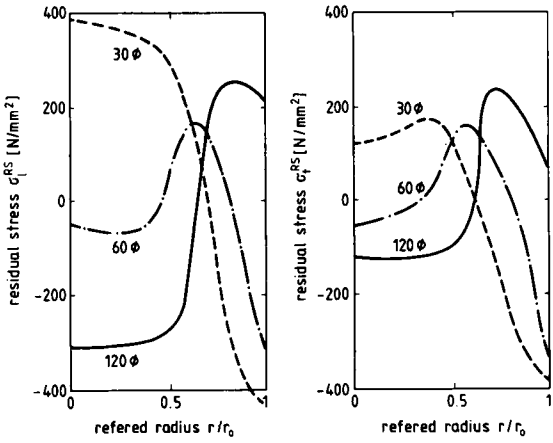


Fig. 24 Calculated distributions of longitudinal and tangential residual stresses versus referred radius of induction hardened steel cylinders with different diameters $\phi = 2\ r_o = 30$, 60 and 120 mm.

with a completed welding procedure are residual stresses and distortions. In regions near the weld usually high tensile residual stresses occur, which may reach magnitudes up to the yield strength of the material being welded. Those tensile residual stresses enhance the failure sensibility of the weld in respect to brittle fracture, fatigue fracture and stress corrosion cracking. The distortions after welding include longitudinal and transverse shrinkages as well as angular or bending distortions, which may influence e.g. the buckling strength of the welded part. Certain process parameters applicable in welding cause smaller (larger) amounts of distortions and larger (smaller) magnitudes of residual stresses. An objective assessment of all preweld manufacturing steps, welding procedures and postweld treatments with respect to their effects on residual stresses and distortions is extremely difficult and needs large experience.

In course of time, however, engineers became familiar with various types of mechanical parts where residual stresses offered benefits with respect to an enhanced service behaviour resp. to a prolonged service life. Especially the fatigue performance of highly stressed parts can be strongly improved by high magnitude surface compressive residual stresses of the 1st kind. On the other hand also various examples of components with deleterious residual stress patterns have been observed, leading to unsafe products, unexpected failures or heavily distorted shapes after machining. Altogether, nowadays the strategy of any proper design should be to utilize the whole capacity of beneficial effects of residual stresses. That means that statically and/or cyclically loaded parts should have residual stresses with desired signs, magnitudes and distributions in specific regions. The optimzied utilization of residual stress states is a challenge of modern materials engineering. It is a tool for material conservation and it seems to be much better than the usual approach, hoping that a sufficient large safety factor would overcome all deleterious effects of residual stresses. In this connection, it is important that for controlling purposes at least surface residual stresses can be monitored with modern measuring techniques fast and not too expensively.

Describing accurately the behaviour of statically loaded components with residual stresses the complete residual and loading stress state must be known. If the

principal axis of both stress states coincide the total stress components can be assumed at any point to be the sum of the loading and the residual stress components

$$\sigma_i^{tot} = \sigma_i = \sigma_i^{LS} + \sigma_i^{RS} \tag{8}$$

with i = 1,2,3. Thus, if triaxial stress states occur, the equivalent stress $\sigma_v$ - e.g. determined according to the distortion energy failure hypothesis - will be

$$\sigma_v = \frac{1}{\sqrt{2}}\sqrt{[(\sigma_1^{LS}+\sigma_1^{RS})-(\sigma_2^{LS}+\sigma_2^{RS})]^2 + [(\sigma_2^{LS}+\sigma_2^{RS})-(\sigma_3^{LS}+\sigma_3^{RS})]^2}$$

$$\overline{+ [(\sigma_3^{LS}+\sigma_3^{RS})-(\sigma_1^{LS}+\sigma_1^{RS})]^2} \tag{9}$$
(9)

where $\sigma_1^{LS}$, $\sigma_2^{LS}$ and $\sigma_3^{LS}$ are principal loading stresses and $\sigma_1^{RS}$, $\sigma_2^{RS}$ and $\sigma_3^{RS}$ are principal residual stresses. In this particular case plastic deformation will occur at that point of the component where the maximum equivalent stress $\sigma_{v,max}$ first reaches the yield strength $R_{eS}$, so that

$$\sigma_{v,max} = R_{eS} \tag{10}$$

As an example in Fig. 25 equivalent stress distributions along the wall of an internally pressurized thick-walled tube are considered. The data hold for a tube with a ratio of outer to inner diameter of $r_a/r_i = 2.0$, with an ideal elastic-plastic material and a yield strength of 1000 N/mm². The curve in the left part of the figure denoted by $\sigma_{V,LS}$ shows the equivalent stress due to an autofrettaging loading pressure of 636 N/mm², which causes inhomogeneous elastic-plastic deformations in the inner part of the tube up to a radius $r = 1.3\ r_i$. This means $(r-r_i)/(r_a-r_i) = 0.3$. After releasing this pressure a triaxial residual stress state occurs with the appertaining equivalent stress $\sigma_{V,RS}$. In the right part of Fig. 25 the distributions of the equivalent stresses of a residual stress free tube ($\sigma_{V,RS\text{-}free}$) and of an autofrettaged tube ($\sigma_V$) are both compared for the same internal pressure of 450 N/mm². The inner walls of the tubes are the failure-critical parts. As can be seen, at this place a much smaller equivalent stress is effective in the autofrettaged tube than in the residual stress free tube. Accordingly, the autofrettaged tube with residual stresses exhibits an increased factor of safety against failure due to plastic deformations.

In ductile material states residual stresses usually have no influence on the fracture strength, because plastic deformations reduce the amount of these stresses. However, in brittle material states the effects of residual stresses have fully to be taken into account if fracture phenomena are considered. Particular benefits of residual stresses for the static loading capability can be reached in the case of notched or cracked parts. The fracture strength of a cracked component will be determined by the fracture toughness $K_{Ic}$ of the material being used and the total crack tip stress intensity factor

$$K_I^{tot} = K_I^{LS} + K_I^{RS} \tag{11}$$

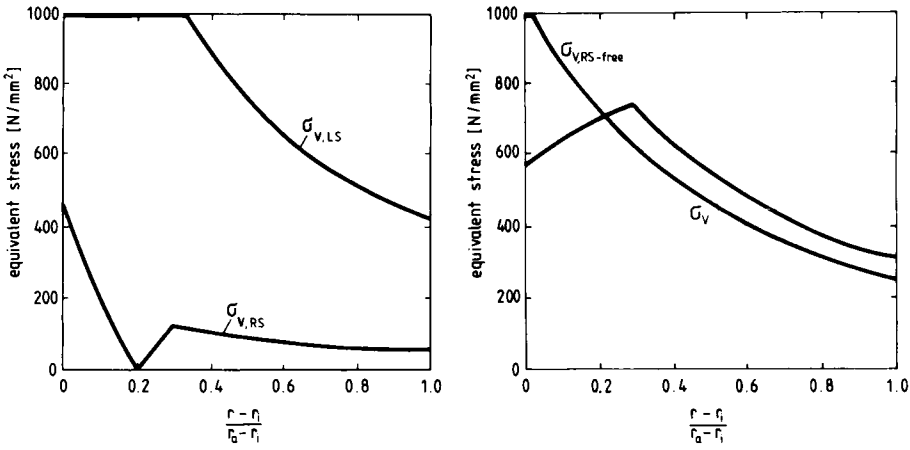


Fig. 25 Distribution of the equivalent stresses along the wall of a thick-walled tube. Left side: Equivalent loading stress $\sigma_{V,LS}$ during autofrettaging with p = 636 N/mm² and equivalent residual stress $\sigma_{V,RS}$ after unloading. Right side: Equivalent loading stress of the autofrettaged tube $\sigma_V$ and equivalent loading stress of a residual stress free tube $\sigma_{V,RS\text{-free}}$ at p = 450 N/mm².

with $K_I^{LS}$ the loading stress intensity factor and $K_I^{RS}$ the residual stress intensity factor. Fracture will occur, if

$$K_I^{tot} = K_{Ic} \tag{12}$$

Obviously the correct assessment of the influence of residual stress patterns on the fracture behaviour of cracked parts under the conditions of linear fracture mechanics requires the knowledge of the residual stress intensity factor $K_I^{RS}$. For material states where the $K_{Ic}$-concept fails the principles of yielding fracture mechanics have to be utilized. However, in these particular cases some uncertainties arise about the consideration of residual stresses on fracture initiation problems. For example the British Welding Institute recommends a pragmatic procedure controlling the effects of residual stresses on the fracture behaviour of weldments with flaws, basing on linear and yielding fracture mechanics [55].

For reasons of completeness it should be further mentioned that residual stresses principally reduce the buckling strength of statically loaded parts with buckling sensitive dimensions [see e.g. 56]. On the other hand compressive residual surface stresses enhance the resistance against stress corrosion cracking of stress corrosion sensitive materials [see e.g. 3,16].

The practically most important area in which residual stresses influence the service behaviour of materials/components/structures is the field of fatigue. In the past several investigations have confirmed that the presence of compressive (tensile) residual stresses at the surface of cyclically loaded materials/components/structures is beneficial (detrimental) to improve fatigue life. Consequently, to such parts, which are expected to have a large resistance against fatigue failure, many designers apply techniques generating compressive residual stresses at and near the surface. Frequently utilized procedures are shot-peening, surface-rolling, induction-hardening, case-hardening, nitriding

and suitable combinations of these treatments. Actually, all methods mentioned improve the high cycle fatigue behaviour of various steels. The observed increase of the endurance level depends on the process variables and can always be contributed to a certain amount of surface compressive residual stresses. In recent years remarkable progress was gained in predicting quantitatively the effects of residual stresses on the fatigue behaviour of surface treated steel parts. Nowadays at least objective concepts can be presented to utilize residual stresses in optimizing the design of various technical components which are fatigue loaded. A typical result [57] to what extent the bending fatigue strength of a low-alloy steel can be increased by case hardening and subsequent shot peening is shown in Fig. 26. The chemo-thermical treatment yields a fatigue strength which is about 4 times greater than that of the normalized steel. By shot-peening a further increase of 6% is realized.

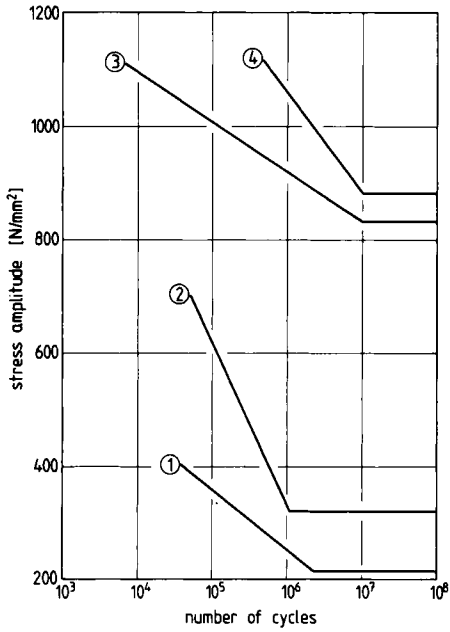


Fig. 26 Woehler-curves of a case hardening steel 16 MoCr 5 (1) normalized state, (2) blind hardened state, (3) case hardened state, (4) case hardened and shot-peened state.

The influence of machining residual stresses on the fatigue behaviour of notched parts is of particular interest. Very recently defined surface residual stress states with different magnitudes and signs of the stress components but the same surface roughness and workhardening states at the notch root of normalized as well as of quenched and tempered steel specimens could be produced [58]. In Fig. 27 the bending fatigue strengths of notched specimens, with different residual stresses in the notch root, are compared with those of smooth specimens with the same surface roughness and workhardening state. As can be seen, notched specimens reveal a smaller residual stress sensitivity of the fatigue strength than smooth specimens. Furthermore, machining which produces high magnitudes of tensile residual stresses, leads to lower fatigue strengths of quenched and tempered than of normalized smooth and notched specimens.

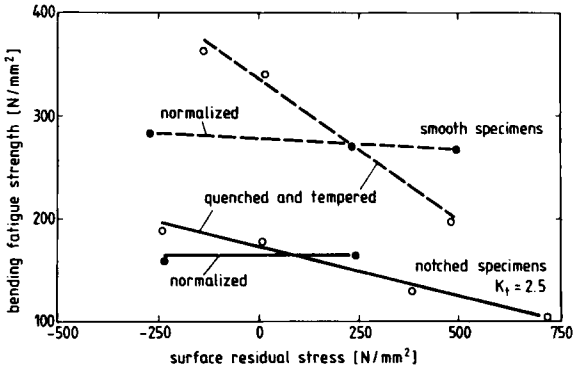


Fig. 27 Influence of machining residual stresses on the bending fatigue strength of differently heat treated smooth (---) and notched (---) specimens of an unalloyed steel with 0.45 wt.-% carbon (stress concentration factor $K_t$ = 2.5).

Experience shows that the beneficial influence of compressive residual stresses on fatigue strength increases up to a certain extent with increasing hardness of the materials being fatigued. This observation is due to the fact that only in high hardness material states residual surface stresses are stable with respect to the applied fatigue loading. It has been verified that the fatigue strength of plain carbon steels with hardness values < 400 HV are unsensitive to residual surface stresses of the 1st kind, which relax nearly completely in course of fatigue loading. In this particular case, however, residual micro stresses enhance the fatigue behaviour. This was undoubtedly demonstrated for milled normalized steel specimens [59]. As can be seen from Fig. 28 annealing - which is combined with the reduction of milling-induced micro stresses - shifts the position of the Woehler-curves to smaller stress amplitude values and reduces the fatigue strength.

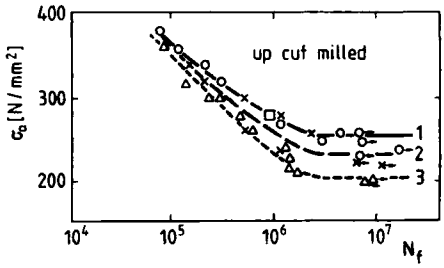


Fig. 28 Woehler-curves of up cut milled specimens of an unalloyed steel with 0.45 wt.-% carbon. 1. up cut milled, 2. after an additional 2h annealing at 500°C and furnace cooling, 3. after an additional 2h annealing at 700°C and furnace cooling.

It is well established that crack growth encloses a more or less large part of the total fatigue life of specimens or structural components [see e.g. 60]. In constant amplitude tests of precracked specimens crack growth can be related to the stress intensity factor ranges

$$\Delta K = K_{max} - K_{min} \quad \text{for } K_{min} > 0 \tag{13}$$

and

$$\Delta K = K_{max} \quad \text{for } K_{min} \leq 0 \tag{14}$$

with $K_{max}$ and $K_{min}$ maximum and minimum stress intensity factor. For much of the specimen life the crack growth rate can be described by the Paris equation [61]

$$\frac{da}{dN} = c\,(\Delta K)^m \tag{15}$$

or the foreman equation [62]

$$\frac{da}{dN} = c^* \frac{(\Delta K)^{m^*}}{(1-\varkappa)\Delta K - K_c} \tag{16}$$

with N the number of loading cycles, a the actual crack length, c and c* resp. m and m* experimentally determined constants, $K_c$ the fracture toughness and $\varkappa = K_{min}/K_{max}$ the stress intensity ratio resp. stress ratio. As a consequence of the inhomogeneous plastic deformations accompanying crack growth, any growing fatigue crack generates its own residual stress field in front of and behind the crack tip. Consequently, also in the case of residual stress free specimens crack growth observations, which agree with the Paris resp. Forman relationship, include the effects of fatigue induced residual stresses. In the middle part of Fig. 29 the distribution of the residual stress component perpendicular to the crack plane of an originally residual stress free RCT-specimen after crack growth up to $a = 16$ mm is shown [63]. The specimen was cyclically loaded with $\Delta K = 920\ N/mm^{-3/2}$ ($\varkappa = 0.05$). The appertaining crack growth rate is sketched as a function of the actual crack length in the upper part of the figure. Ten overloading cycles with $\Delta K_1 \simeq 1610\ N/mm^{-3/2}$ ($\varkappa = 0.03$) change the residual stress state near the crack tip in the manner illustrated in the lower part of the figure. In front of the crack an extended area with compressive residual stresses has been developed which retards the crack growth rate during succeeding cyclic loading with $\Delta K_o$, as can be seen from the appertaining data presented in the upper part of the figure.

Since structural parts mostly contain residual stress fields due to technological treatments, it is to be expected that compressive residual stresses retard fatigue crack growth, while tensile residual stresses may act accelerating. To take quantitatively account of the influence of residual stresses on fatigue crack growth, appropriate values of the residual stress intensity factors $K^{RS}$ for the particular crack shapes and crack plane residual stress must be known. Then the maximum and minimum loading stress intensities $K_{max}^{LS}$ and $K_{min}^{LS}$ can be superimposed on $K^{RS}$ as exemplarily illustrated for compressive residual stresses and $K_{min}^{LS} + K^{RS} > 0$ in the upper part and $K_{min}^{LS} + K^{RS} \leq 0$ in the lower part of Fig. 30. In the first case mentioned the effective cyclic stress intensity range

$$\Delta K_{eff} = K_{eff,max} - K_{eff,min} = \Delta K^{LS} \tag{17}$$

is independent of the residual stress intensity $K^{RS}$, whereas the effective stress ratio $\varkappa_{eff}$ depends on $K^{RS}$. Therefore only a weak influence of residual stresses on fatigue crack growths is to be expected. However, in the second case the effective cyclic stress intensity factor range is given by

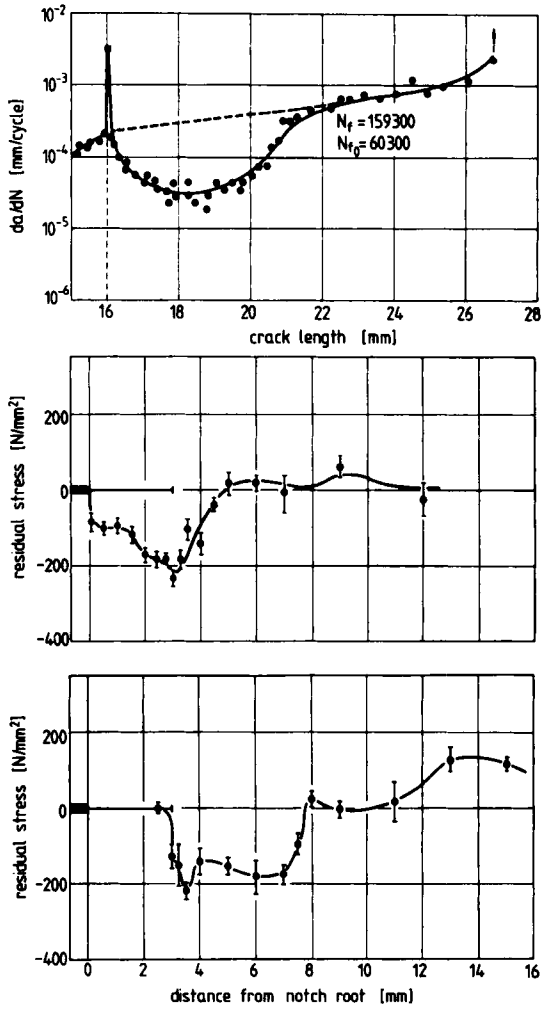


Fig. 29 Crack growth rate versus crack length of a RCT specimen (material: plain carbon steel with 0.22 wt.-% carbon) without (---) and with (——) overloading after reaching a crack length of 16 mm (upper part of the figure). At the middle (bottom) of the figure distributions of the residual stresses perpendicular to the ligament before (after) overloading are sketched.

$$\Delta K_{eff} = K_{max}^{LS} + K^{RS} = K_{eff,max} \tag{18}$$

which strongly depends on $K^{RS}$. Consequently, a more pronounced effect of residual stresses is anticipated. Actually however, the residual stress intensity factors $K^{RS}$, the effective stress intensity range $\Delta K_{eff}$ as well as the effective stress intensity ratios $H_{eff}$ change with crack growth. Therefore, more

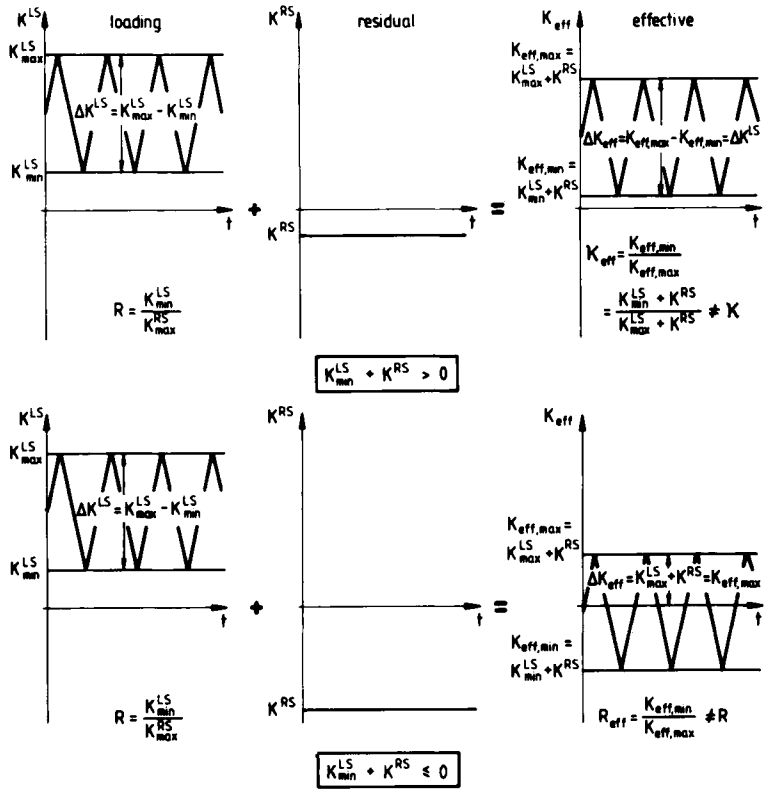


Fig. 30 Consequences of superposition of loading and residual stresses on the effective stress intensities of cracked specimens.

complicated considerations are necessary. The variation of $K^{RS}$ along the expected crack growth direction must be known for appropriate predictions of actual crack growth rates. As an examaple Fig. 31 shows schematically crack rate curves for edge-cracked specimens with tensile (compressive) residual stresses in the outer part and compressive (tensile) residual stresses in the middle part subjected to tension-to-tension loading. For comparison also the crack rate curve of a residual stress free specimen is drawn, which follows Eq. 15. Initial crack growth in the tensile (compressive) part of a residual stress field yields a positively (negatively) bent crack growth rate versus $\Delta K$ curve, as illustrated by the dashed (dotted) line [64]. Recent investigations of the influence of welding residual stresses on the fatigue crack growth in a structural steel seem to be in agreement with these considerations [65].

Finally, it should be mentioned, that fatigue crack growth can even completely be stopped, if suitable residual stress fields are generated in front of an extending crack. Figure 32 comprises results of corresponding observations. At both sides of a RCT-specimen hardness indentations were produced, as illustrated schematically at the right side of the middle part of the figure. The specimen thickness was 3 mm. Position and schematical contour of the hardness indentation are noted. At the left side of the middle part of the figure the crack growth rate is drawn versus crack length, if the specimen is cyclically tension-to-tension loaded with $\Delta\sigma$ = 21 N/mm². At first, an increase

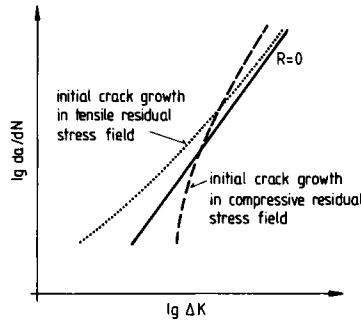


Fig. 31 Crack rate curves (lg da/dN, lg ΔK-curves) of residual stress free cracked specimens (H = 0) and residually stressed cracked specimens with initial crack growth in tensile resp. compressive residual stress fields.

of crack growth rate is observed with increasing crack length. However, if the crack tip reaches the compressive residual stress field the crack growth rate drops off and finally goes to zero at a crack length of about 18.3 mm. Then, the residual stress distribution sketched in the lower part of the figure has been developed.

## CONCLUDING NOTES

This introductory paper is meant as an attempt to give a feeling for the actual state of knowledge in the broad field of residual stresses. Of course, thereby not all areas could be mentioned which are of scientific and/or technological interest. Nevertheless it was tried to sketch the complexity and breadth of this fascinating field and to indicate some recent successes and evolutions. The frequent reference to own investigations in this paper should be seen as a decision of convenience. This was done with full respect to the work of all colleagues having contributed to the present state of knowledge about residual stresses.

However, in spite of the progresses and developments achieved in recent years, there still exists a large number of unsolved problems of scientific and technological importance which should be solved by future theoretical and/or experimental contributions. The following chapters of this handbook, which present up to date and detailed informations about selected parts of the sector of residual stresses, should desirably stimulate scientists and engineers to do further successful work in this field.

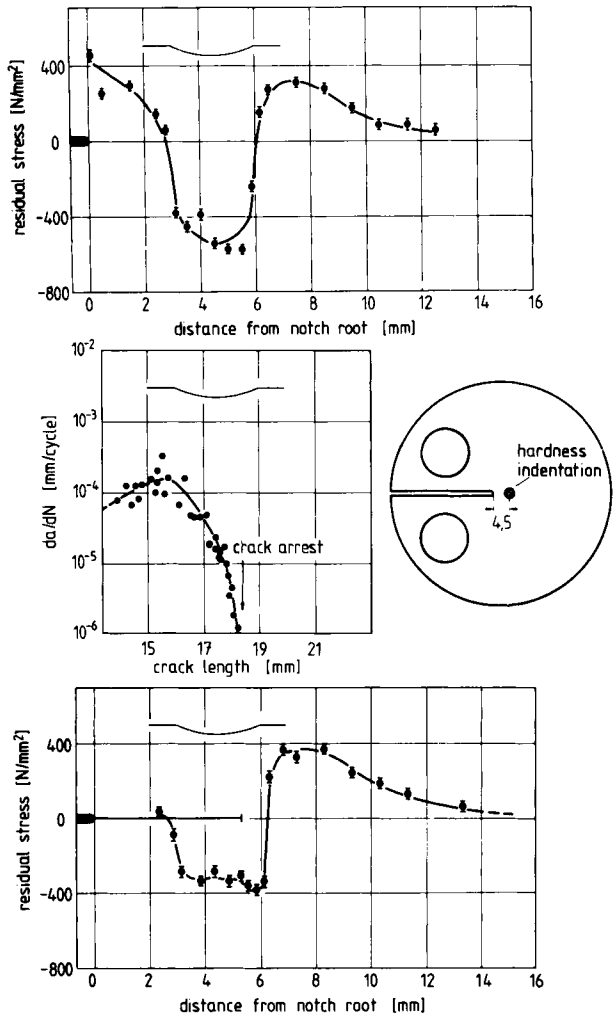


Fig. 32 Fatigue crack extension in residual stress fields produced at RCT-specimens by hardness indentations.

REFERENCES

[1] Neumann, F. E. (1841) Die Gesetze der Doppelbrechung des Lichts in comprimiertenj und ungleichförmig erwärmten unkrystallinischen Körpern, Abh. Königl. Akad. Wiss. Berlin, 2. Theil, p. 1.

[2] Baldwin Jr., W. M. (1949) Residual Stresses in Metals, Proc. ASTM 49, p. 539.

[3] Rassweiler, G. M. and W. L. Grube (ed.) (1959) Internal Stresses and Fatigue in Metals, Elsevier Publi. Comp., Amsterdam/London/New York/ Princeton.

[4] Macherauch, E. (1979) Neuere Untersuchungen zur Ausbildung und Auswirkung von Eigenspannungen in metallischen Werkstoffen, Z. Werkstofftechn., 10, p. 97.
[5] Van de Walle, L. J. (ed.) (1981) Residual Stress for Designers and Metallurgists, ASM, Metals Park, Ohio.
[6] Kula, E. and V. Weiss (ed.) (1982) Residual Stress and Stress Relaxation. Proc. 28th Sagamore Army Materials Research Conference, Plenum Press, New York/London.
[7] Hauk, V. and E. Macherauch (ed.) (1982) Eigenspannungen und Lastspannungen, Beiheft HTM, Carl Hanser Verlag, München/Wien.
[8] Throop, J. F. and H. S. Reemsnyder (1982) Residual Stress Effects in Fatigue, ASTM, STP 776.
[9] Macherauch, E. and V. Hauk (ed.) (1983) Eigenspannungen, Enstehung-Messung-Bewertung, Deutsche Gesellschaft für Metallkunde e.V., Oberursel. Band 1 und 2.
[10] Macherauch, E. (1984) Residual Stresses, in Sih, G.C., E. Sommer and W. Dahl (ed.). Application of Fracture Mechanics to Materials and Structures, Martinus Nijhoff Publishers, The Hague/Boston/Lancaster, p. 157.
[11] Macherauch, E., H. Wohlfahrt and U. Wolfstieg (1973) Zur zweckmäßigen Definition von Eigenspannungen HTM, 28, p. 201.
[12] Yu, H. J. and E. Macherauch (1980) Calculation of quenching stresses with and without transformation effects, in [6], p. 483.
[13] Bock, H., H. Hoffmann and H. Blumenauer (1976) Mechanische Eigenschaften von Wolframkarbid-Kobalt-Legierungen, Technik, 31, p. 47.
[14] Li, J. C. M. (1963) Theory of Strengthening by Dislocation Groupings in G. Thomas, J. Washburn (ed.), Electron Microscopy on Strength of Crystals, Interscience Publ., New York/London, p. 713.
[15] Peiter, A. (1966) Eigenspannungen I. Art, M. Triltsch Verlag, Düsseldorf.
[16] Tietz, H.-D. (1983) Grundlagen der Eigenspannungen, VEB Deutscher Verlag Grundstoffindustrie, Leipzig.
[17] Ruud, C. O. (1981) A review of non-destructive methods for residual stress measurement, J. Met., p. 35, July.
[18] James, M. R. and O. Buck (1980) Quantitative nondestructive measurement of residual stresses, Solid State Sci., p. 61, August.
[19] Ruud, C. O. (1982) A review of selected non-destructive methods for residual stress measurement, NDT International, p. 15, February.
[20] Wolf, H. and W. Böhm (1971) Das Ring-Kern-Verfahren zur Messung von Eigenspannungen und seine Anwendung bei Turbinen und Generatorwellen, Arch. Eisenhüttenwes., 42, p. 195.
[21] Böhm, W., E. Stucker and H. Wolf (1980) Grundlagen und Anwendungsmöglichkeiten des Ring-Kern-Verfahrens zum Ermitteln von Eigenspannungen, Meßtechn. Briefe, 16, p. 36 (Heft 2) and p. 66 (Heft 3).
[22] Macherauch, E. and P. Müller (1961) Das $\sin^2\psi$-Verfahren der röntgenographischen Spannungsmessung, Z. angew. Phys., 13, p. 305.
[23] Macherauch, E. and U. Wolfstieg (1977) A Modified Diffractometer for X-ray Stress Measurements, in H. F. McMurdie, C. S. Barrett, J. B. Newkirk, C. O. Ruud (ed.), Advances in X-Ray Analysis, Vol. 20, p. 369.
[24] Maurer, G. (1985) unpublished results, IWK I, Karlsruhe University.
[25] Kolb, K. and E. Macherauch (1965) Die Eigenspannungsausbildung in verformten Stählen, Arch. Eisenhüttenwes., 36, p. 8 and p. 19.
[26] Gründler, O., W. Mitter and G. Wiedner (1980) Vergleichende Eigenspannungsmessungen an abgeschreckten Nickelstahl-Zylinder, Technisches Messen, Heft 3, p. 93.
[27] Brinksmeier, E., J. T. Cammett, W. König, P. Leskovar, J. Peters and H. K. Tönshoff (1982) Residual Stresses - Measurement and Causes in Machining Processes, Annals of the CIRP, Vol. 31/2, p. 491.
[28] Hoffmann, J., H. Neff, B. Scholtes and E. Macherauch (1983) Flächenpolfiguren und Gitterdeformationspolfiguren von texturierten Werkstoffzuständen, Härterei-Techn. Mitt., 38, p. 180.
[29] Hauk, V. and G. Vaessen (1983) Röntgenographische Spannungsermittlung an texturierten Stählen, in [9] Band 2, p. 9.

[30] Barral, M., J. M. Sprauel and G. Maeder (1983) Stress Measurements by X-ray Diffraction on Textured Material Characterised by its Orientation Distribution Function, in [9] Band 2, p. 31.
[31] Hauk, V., D. Berlach and H. Sesemann (1975) Über nichtlineare Gitterebenen-Abstandsverteilungen in Stählen, ihre Entstehung, Berechnung und Berücksichtigung bei der Spannungsermittlung, Z. Metallkde., 66, p. 734.
[32] Dölle, H. and V. Hauk (1978) Einfluß der mechanischen Anisotropie des Vielkristalls (Textur) auf die röntgenographische Spannungsermittlung, Z. Metallkde., 69, p. 410.
[33] Prümmer, R., Residual Stresses due to Electron Beam Butt Welding of a 0.32 % Plain Carbon Steel, J. Soc. Mat. Sci., Japan, 17, p. 1066.
[34] Pintschovius, L., V. Jung, E. Macherauch, R. Schäfer and O. Vöhringer (1982) Determination of residual stress distribution in the interior of technical parts by means of neutron diffraction, in [6], p. 467.
Pintschovius, L., V. Jung, E. Macherauch and O. Vöhringer (1983) Residual Stress Measurements by Means of Neutron Diffraction, Mat. Sci. Eng., 61, p. 43.
[35] Krawitz, A. D., J. E. Brune and M. J. Schmank (1982) Measurement of stress in the interior of solids with neutrons, in [6], p. 139.
[36] Allen, A., C. Andreani, M. T. Hutchings and C. G. Windsor (1981) Measurement of internal stress within bulk material using neutron diffraction, NDT International, p. 249, October.
[37] Schneider, E. and K. Goebbels (1983) Zerstörungsfreie Bestimmung von Eigenspannungen mit Ultraschallverfahren, in [9], Band 2, p. 69.
[38] Attebo, E. and T. Ericsson (ed.) (1984) Calculation of Internal Stresses in Heat Treatment of Metallic Materials, May 23-25, Vol. 1-2, Linköping, Sweden.
[39] Masubuchi, K. (1980) Analysis of Welded Structures, Pergamon Press, Oxford/New York/Toronto/Sydney/Paris/Frankfurt.
[40] Ericsson, T., B. Hildenwall (1982) Thermal and Transformation Stresses, in [6], p. 19.
[41] Denis, S., J. C. Chewier, A. Simon and G. Beck (1979) Determination de l'influence d'une transformation martensitique sur l'évolution des contraintes au cours de la trempe, Mem. Sci. Rev. Met., 76, p. 221.
[42] Burnett, J. A. (1977) Calculation of elastic-plastic stresses in quenched cylinders by FEM, PhD-Thesis, University of Akron (Ohio).
[43] Yu, H. J., U. Wolfstieg and E. Macherauch (1978) Berechnung von Eigenspannungen mit Hilfe eines speziellen Finite-Element-Programms, Arch. Eisenhüttenwes., 49, p. 499.
[44] Inoue, T. and B. Rainecki (1978) Determination of thermal hardening stress in steels by use of thermoplastic theory, J. Mech. Phys. Sol., 26 p. 187.
[45] Rammerstorfer, F. G., D. F. Fischer, H. Steiner, W. Mitter and G. Schatzmayr (1980) Zur Bestimmung der Eigenspannungen in Bauteilen bei Wärmebehandlung mit Phasenumwandlung, DGM-Symposium Bad Nauheim, p. 181.
Mitter, W., F. G. Rammerstorfer (1983) Finite-Element-Modell zur Bestimmung der Umwandlungsplastizität bei Eigenspannungsberechnungen, in [9], Band 1, p. 239.
[46] Sjöström, S. (1983) Berechnung von Abschreckeigenspannungen in Stahl, in [9], Band 1, p. 155.
[47] Denis, S., A. Simon and G. Beck (1983) Analysis of the thermomechanical behavior of steel during martensitic quenching and calculations of internal stresses, in [9], Band 1, p. 211.
[48] Rybicki, E. F., D. W. Schmueser, R. B. Stonesifer, J. J. Groom and H. W. Misher (1978) A finite element model for residual stresses and deflections in girth-butt welded pipes, Trans. ASME J. Press. Vessel Techn., 100, p. 256.
[49] Rybicki, E. F. and R. B. Stonesifer (1979) Computation of residual stresses due to multipass welds in piping systems, Trans ASME J. Press. Vessel Techn., 101, p. 149.

[50] Rybicki, E. F. and R. B. Stonesifer (1981) Stress intensity factors due to residual stresses in thin-walled girth-welded pipes, Trans. ASME J. Press. Vessel Techn. 103, p. 66.
[51] Pu, S. L. and M. A. Hussain (1981) Residual stress redistribution caused by notches and cracks in a partially autofrettaged tube, Trans. ASME J. Press, Vessel Techn., 103, p. 302.
[52] Burnett, J. A. (1981) Prediction of stresses generated during the heat treating of case carburizing parts, in [5], p. 51.
[53] Brückner, V., W. Schuler and H. Walter (1983) Untersuchungen zum Eigenspannungszustand beim induktiven Randschichthärten, in [9], Band 1, p. 293.
[54] Melander, M. (1983) Computer calculations of residual stresses due to induction hardening, in [9], Band 1, p. 309.
[55] Harrison, J. D., M. G. Dawes, G. L. Archer and M. S. Kamath (1979) The COD approach and its application to welded structures, ASTM STP 688, p. 606.
[56] Thürlimann, B. (1957) Der Einfluß von Eigenspannungen auf das Knicken von Stahlstutzen, Schweizer Archiv., p. 388, December.
[57] Schreiber, R., H. Wohlfahrt and E. Macherauch (1978) Der Einfluß des Kugelstrahlens auf das Biegewechselverhalten von normalgeglühtem (blindgehärtetem und einsatzgehärtetem) 16 MnCr 5, Arch. Eisenhüttenwes., 48, p. 649, p. 653; 1977; 49, p. 37, 1978.
[58] Hoffmann, J. E. (1983) Der Einfluß fertigungsbedingter Eigenspannungen auf das Biegewechselverhalten von glatten und gekerbten Proben aus Ck 45 in verschiedenen Werkstoffzuständen, Dr.-Ing. Dissertation, Karlsruhe University.
[59] Syren, B., H. Wohlfahrt and E. Macherauch (1976) The influence of residual stresses and surface topography on bending fatigue strength of machined Ck 45 in different heat treatment conditions, Proc. 2nd Int. Conf. Mech. Beh. Mat., Special Vol., Boston, p. 807.
[60] Munz, D. (ed.) (1985) Ermüdungsverhalten metallischer Werkstoffe, DGM-Informationsgesellschaft, Verlag, Oberursel.
[61] Paris, P. C., M. P. Gonese and W. E. Anderson (1961) A rational analytical theory of fatigue, The Trend in Engineering, Univ. of Washington, 13, p. 9.
[62] Forman, R. G., V. E. Kearney and R. M. Engle (1967) Numerical analysis of crack propagation in cyclically loaded structure, J. Basic Engin., 89, p. 459.
[63] Welsch, E. (1985) Der Einfluß rißspitzennaher Eigenspannungen auf die Ausbreitung von Ermüdungsrissen, Dr.-Ing. Dissertation, Karlsruhe University.
[64] Parker, A. P. (1982) Stress intensity factors, crack profiles and fatigue crack growth rates in residual stress fields, in [8], p. 13 and p. 249.
[65] Glinka, G. (1979) Effect of residual stresses on fatigue crack growth in steel weldments under constant and variable amplitude loads, in C. W. Smith (ed.), Fracture mechanics, ASTM STP 677, p. 198.